Theory for Intermetallic Phase Growth Between Cu and Liquid Sn-Pb Solder Based on Grain Boundary Diffusion Control

MATT SCHAEFER,[1] RAYMOND A. FOURNELLE,[1] and JIN LIANG[2]

1.—Materials Science Program, Marquette University, Milwaukee, WI 53201-1881. 2.—Rockwell Automation (Allen-Bradley) 1201 S. Second Street, Milwaukee, WI 53204-2496

Kinetics of phase formation during interdiffusion in solid-liquid diffusion couples are influenced by the morphology of the intermediate compound layer. In some cases, an intermediate compound layer is formed which has very fine grain size. This condition favors grain boundary diffusion as the predominant mechanism for transport through the layer. In systems where grain coarsening occurs, the coarsening kinetics will influence the interdiffusion kinetics. In addition, for some solid-liquid systems, a grain boundary grooving effect is observed which leads to a highly nonuniform layer thickness; the layer is thinner where the liquid phase penetrates the grain boundaries. As a consequence of the grooving effects, the diffusion path through the layer is shorter along the grain boundaries. This differs from standard interdiffusion models which assume that the diffusion distance is equal to the average layer thickness. A model for growth kinetics of an intermediate compound layer is presented for the case where grain boundary diffusion is the predominant transport mechanism. The model includes the geometric effects caused by grain boundary grooving. The model predicts layer growth which follows a $t^{1/3}$ dependence on time t. Experimental data for intermetallic growth between copper and 62Sn-36Pb-2Ag solder exhibit a $t^{1/4}$ dependence on time t. If experimental data are interpreted in terms of the grain boundary diffusion control model presented in this paper, the activation energy for grain boundary diffusion is 27 kJ/mole.

Key words: Cu-Sn intermetallics, grain boundary diffusion, grain coarsening, intermetallic compound growth, Sn-Pb-Ag solder

INTRODUCTION

Understanding solder-substrate reactions is an important aspect of solder joint processing. The intermetallic layer which develops between Sn containing solders and Cu substrates is a necessary part of a sound metallurgical bond. However, excessive intermetallic may degrade the fatigue or fracture strength of a solder joint.[1–4] Also, the morphology of the intermetallic layer after soldering influences the subsequent solid-state aging behavior of the joint.[5] The focus of this paper is on modeling the intermetallic growth during the soldering process when a copper substrate is in contact with molten tin-lead solder.

Much of the work in the literature deals with experimental aging of solder-substrate couples below the melting point of the solder.[6–9] For Cu-Sn and related systems, the typical morphology reported for the intermetallic layer is a relatively planar, two-phase structure: ε-phase (Cu_3Sn) near the Cu and η-phase (Cu_6Sn_5) near the solder. The η-phase is the majority component, grows more rapidly, and appears first during the initial stages of growth. One study, included inert markers in the diffusion couples. Movement of these markers toward the Sn-rich side of the couple indicated that Sn was the more rapidly diffusing species.[6]

Diffusion control models for intermetallic layer growth have been developed.[10,11] These models are based on a fairly detailed analysis of diffusion through the intermetallic layers. Basic assumptions for these models include:

- Diffusion coefficients are independent of composition,
- Local equilibrium is maintained at the phase boundaries,
- Phase boundaries are flat and parallel, and
- Volume diffusion through the layer is the predominant mechanism of diffusion.

Experimental growth rate studies for solid state

(Received February 18, 1998; accepted June 1, 1998)

systems show that intermetallic layers exhibit nearly a parabolic dependence of layer thickness (x) vs time (t); i.e., $x = k*t^{0.5}$. However, most of these papers report deviations from parabolic behavior in the regime where intermetallic layers are relatively thin.[12–14] In a numerical model, this "enhanced diffusion" may be empirically accounted for by introducing a variable diffusion coefficient which is a function of layer thickness.[10] One possible justification for using the variable diffusion coefficient is that thin (fine grained) layers may favor grain boundary diffusion as the predominant transport mechanism. Correlation of numerical results with experimental studies shows that these models are useful for predicting the aging behavior of solid-solid couples over fairly long aging times.[12,13]

The above models do not presuppose solid or liquid reactants; however, the layer geometry assumed for these models does not fit the observed morphology of layers that develop in solid-liquid couples. There are three important differences.[9,15–20] First, layers that develop during soldering are generally much thinner than the layers reported in the solid state studies, thus, the "enhanced diffusion" regime described above encompasses the entire soldering process. Second, the grain size within the layers is very fine—on the order of a micron or less. As a result, the effect of grain boundary diffusion will be more pronounced. Third, the η-phase layer exhibits a distinctive scalloped morphology. Copper samples in contact with liquid Sn for as little as 10 s showed the η-phase as rounded grains on the copper. In between these grains were channels of unreacted Sn or solder. It is generally assumed that these channels are associated with grain boundaries in the η-phase layer. Formation of the channels may be attributed to a grain boundary grooving phenomenon. The presence of these grooves shortens the diffusion distance along grain boundaries and, thus, further enhances the effect of grain boundary diffusion through the layer.

An additional feature of intermetallic in solid-liquid couples is the observation that the grain size within the η-phase coarsens as the layer grows thicker.[17–21] Since the grain boundaries may play a dominant role for diffusion, this coarsening effect is closely coupled with the rate of transport through the layer.

Layer growth kinetics for solid-liquid couples are significantly faster compared to growth kinetics for solid-solid couples. Growth rates for layers in solid-liquid couples are about an order of magnitude faster than would be predicted for a solid state system with the same average layer thickness.[15,16,22] In addition, the time dependence for layer growth during soldering is subparabolic. Experiments indicated an exponent between n = 0.21 and n = 0.37 when growth data were fit to a growth law of the form: $x = k*t^n$, where x = η-phase layer thickness or total layer thickness and t = time.[15,17,18,21,22] If this were a standard diffusion controlled process, the expected time exponent would be n = 0.5. Therefore, the numerical results clearly indicate that the layer growth does not follow the standard interdiffusion model. These differences are likely related to the distinctive layer morphology observed in solid-liquid systems.

Kim and Tu[20] have developed a model for the growth of scalloped intermetallic layers between Cu and molten Sn-Pb solder which assumes that the scalloped grains coarsen by a ripening reaction driven by the Gibbs-Thompson effect and that Cu dissolves into the molten solder along liquid channels between the scallops. This model predicts a 1/3 power dependence of the mean scallop radius and, hence, layer thickness on time. This model requires that the liquid channels extend through the η-phase layer to the ε-phase layer. With the exception of very short reflow times, this assumption is not generally supported by metallographic observations in the literature.[9,16–18]

Lea has outlined a simple model for layer growth in solder-substrate couples.[23] In this paper, Lea's simple model will be modified in order to accommodate the unique features of layer growth between a liquid solder and a solid substrate. This paper examines:

- The influence of the geometry (scalloped η-phase),
- The growth of intermetallic during soldering under isothermal conditions and the contribution of grain boundary diffuison, and
- The effects of grain coarsening.

THEORY

Growth of an intermetallic layer in solid-liquid couples under conditions relevant to soldering is a complex problem. It involves the net effect of several interrelated phenomena: diffusion through the layer via bulk and grain boundary diffusion, grain boundary grooving, grain coarsening, and dissolution into the molten solder. Several physical and morphological characteristics which are distinct for the case of solid-liquid interdiffusion couples have important ramifications for the analysis of layer growth in these systems. First, the diffusion analysis must be modified to account for scalloped morphology of the intermetallic layer. This layer morphology determines the geometry for the analysis of diffusional flux through the layer. Second, grain boundary diffusion may play an important role in the diffusional flux through the layer. The diffusion model must account for this. Third, coarsening of the intermetallic grains will influence the diffusion rate. Coarsening decreases the number of grain boundaries available as rapid diffusion paths through the layer. In addition, coarsening may change the geometry of the scalloped layer. A fourth phenomena exists but will not be included in the analysis method presented in this paper. In the initial stages of layer growth, there is a net flux of Cu from the substrate into the liquid solder. This is the result of a dissolution reaction at the solder-intermetallic interface.[21,23] This reaction ceases when the solder approaches saturation. Only the case of soldering with saturated solder will be considered in this paper. In the present work, the analysis of each individual phenomenon will be based on a fairly

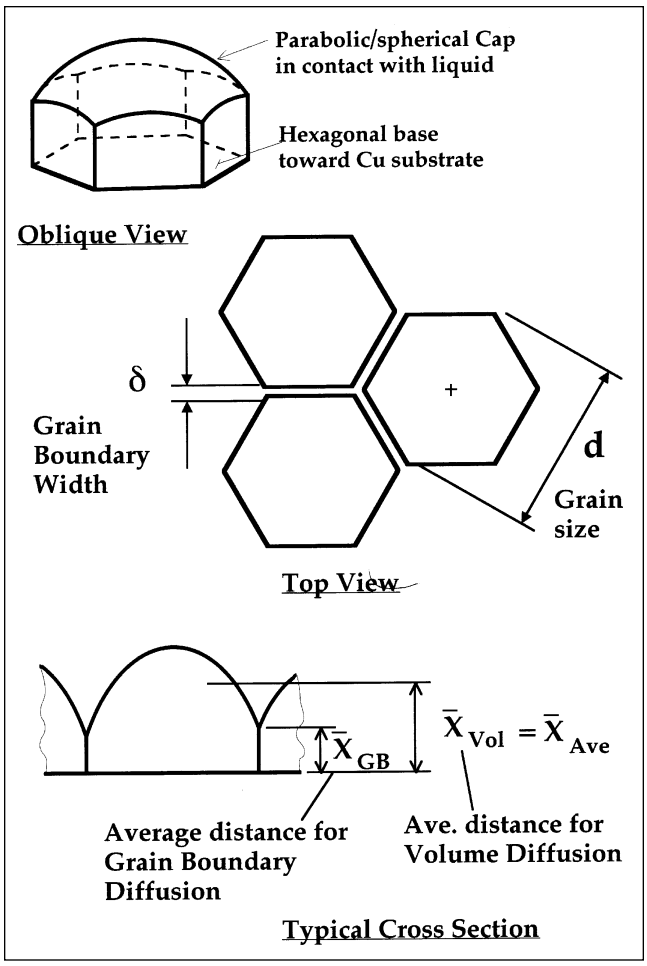

Fig. 1. Geometric model of scallop shaped grains which comprise the Cu_6Sn_5 layer. Some relevant dimensions used in the diffusion model are shown.

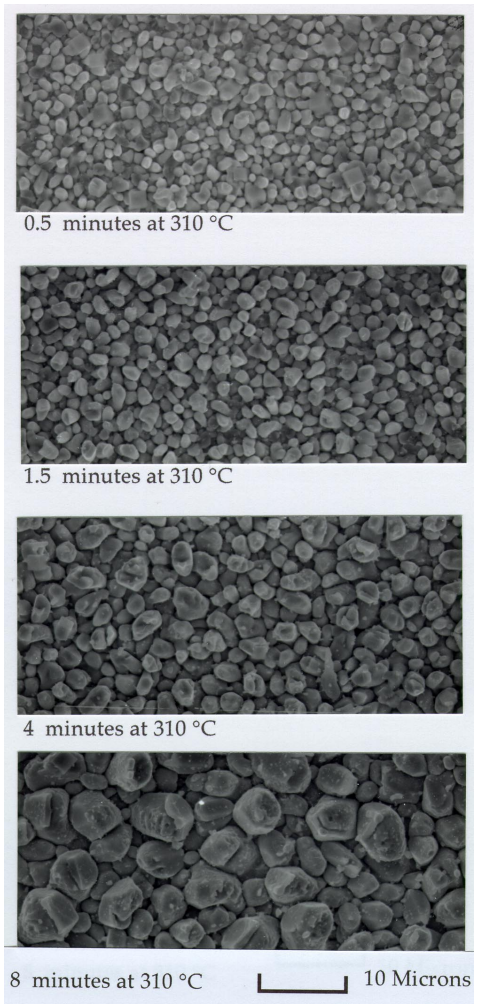

Fig. 2. SEM photos showing exposed η-phase scallops revealed by chemically removing the solder.

simple model. Despite these necessary simplifications, the numerical method presented will provide a useful framework for developing a detailed model of intermetallic layer growth.

Assumptions for the Physical Model

The initial condition for the growth model is the point where a continuous intermetallic layer is established. Nucleation and growth of individual grains occurs very rapidly. Experimental observations with Sn and Sn-Pb solders indicate that the layer is continuous after as little as 10 s.[9,17,18] Once a continuous layer is established, additional growth requires diffusion of the reacting species (Sn and/or Cu) through the intermetallic layer.

The grain structure of the intermetallic layer has a key influence on diffusion rate through the layer. It is assumed that each scallop of the η-phase layer corresponds to one grain. Throughout this paper the terms 'η-phase scallop' and 'η-phase grain' will be used interchangeably. This assumption is reasonable, in particular for the early stages of soldering. The η-phase grains are assumed to have a hexagonal shaped base toward the Cu substrate and a rounded top (spherical or parabolic) in contact with the liquid solder (Fig. 1). This correlates with scanning electron microscopy (SEM) photographs (Fig. 2) which show that most of the scallops have 5, 6, or 7 near neighbors. In addition, these photos show the presence of the deep channels between grains. These channels appear to be deepest at triple points where three grains meet. Both of these characteristics follow the hexagonal-base/spherical-cap geometric model.

One limitation of this model is that it assumes a uniform grain size; whereas, the actual layers consist of a variety of grain sizes. Another limitation, is that a few of the larger grains have shapes which are not hexagonal, rather, they are more elongated. For short reflow times, the assumptions of hexagonal grains, uniform size, and spherical caps seem to be very good. For longer reflow times, there is a divergence in scallop sizes and shapes; however, the above assumptions still fit the majority of the scallops and should provide a reasonable approximation for these layers.

The η-phase layer consists of a monolayer of grains thus the average grain size perpendicular to the layer is equal to the average thickness of the layer. Experimental observations indicate that the typical lateral

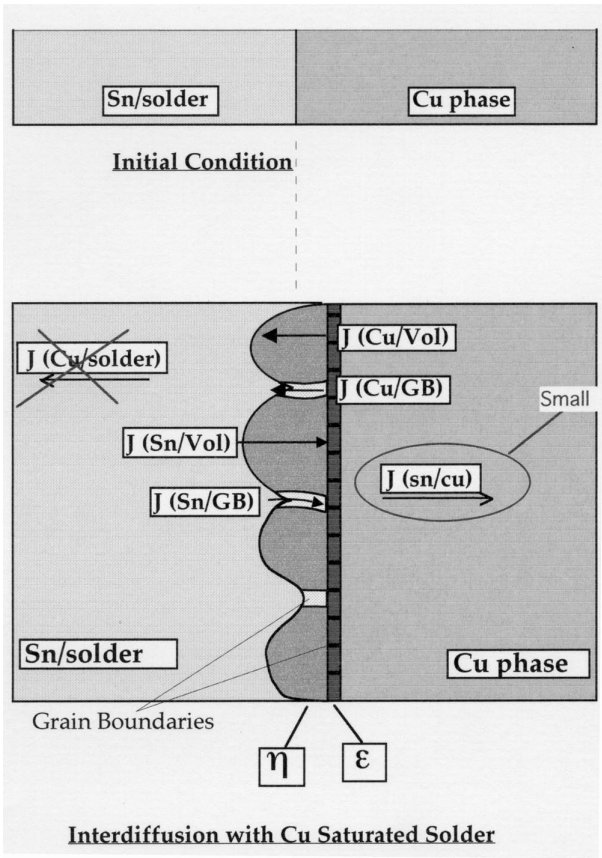

Fig. 3. A schematic model of the possible fluxes due to interdiffusion in the molten solder/Cu couple.

grain size is nearly equal to the thickness (i.e., grains are approximately equiaxed). Experimental data from Kim, Liou, and Tu[15,19,20] show that as η-phase scallops grow from 1.3 microns (10 s soldering time) to over 10 microns (40 min soldering time) the average area covered by each scallop grows from 2.5 to 67 μm^2. Thus, the height-to-base ratio changes from roughly 0.8 to 1.2. As a first approximation, it will be assumed for this analysis that the grains remain equiaxed (height:base = 1).

The ε-phase layer consists of a monolayer of grains. In most experimental observations, the layer is nearly uniform in thickness. Though it is not always planar, it is much closer to planar than the η-phase layer. Though ε-phase is present even after short soldering times[7,18,20] it comprises only a small fraction of the total intermetallic layer even after longer soldering times.[16,20,22] Therefore, for an approximate analysis of layer growth rate, the predominant reaction is assumed to be diffusion through the η-phase layer. In essence, the thin layer of ε-phase ahead of the advancing η-phase boundary will be treated as one step in the interfacial reaction:

$$5Sn + 6Cu \xrightarrow{\varepsilon} Cu_6Sn_5.$$

Diffusion Model

Most of the fundamental aspects of a standard diffusion limited growth model (which leads to the standard parabolic growth law, $X = k\,t^{1/2}$) will be applied to the present system.[25] Primary assumptions for the model include:

- Diffusion through the layer is the slowest step and thus is the rate limiting mechanism,
- The interphase boundaries are in local equilibrium so the phase compositions at the boundaries are constant,
- Flux into the terminal phases is negligible, (this is justified due to slow diffusion into the copper and the assumption that the liquid phase is saturated with Cu), and
- The diffusion coefficients are independent of composition.

It will be assumed that flux through the layer occurs only perpendicular to the layer (Fig. 3). Lateral flux due to the three-dimensional geometry or due to leakage from the grain boundaries into the grains will be neglected. It will also be assumed that the curvature of the η-phase scallops has no effect on the composition of the η-phase at the η-solder interface.

By applying this one dimensional approximation, the flux across the η-phase layer is given by Fick's first law:

$$J = -D\frac{dC}{dX} \tag{1}$$

where, D is the appropriate diffusion coefficient. This may be rewritten in discrete form based on assumptions (2) and (4) above:

$$J = -D\frac{\Delta C}{\Delta X} \tag{2}$$

For practical purposes, growth rate is usually controlled by diffusion of the faster diffusing species. The literature suggests that for A_mB_n intermetallic compounds with stoichiometric ratios near one (i.e., $\frac{m}{n} \approx 1$) the element with the lower melting point is the more rapid diffuser. For the specific case of Cu_6Sn_5, this observation is backed up by experimental diffusion studies in which marker movement in a solid state diffusion couple indicated that Sn was the more rapidly diffusing species.[6] As a result, it can be assumed that continued growth of η-phase intermetallic will largely be controlled by the rate of Sn diffusion through the layer.

The total flux through the η-phase layer is the sum of grain boundary and volume diffusion contributions. For the η-phase layer, the flux resulting from volume diffusion may be obtained by applying Fick's law and taking the average layer thickness (X_{Ave}) as an approximation for the average diffusion distance.

$$J_\eta^{VOL} = -D_\eta^{VOL}\frac{\Delta C}{X_{Ave}} \tag{3}$$

In order to determine the contribution of grain boundary diffusion, a similar calculation is required; however, three modifications must be made. First, it must be noted that due to the scalloped grains (grain boundary grooving), the average diffusion distance along grain boundaries ($X_{Ave\ GB}$) is *shorter* than the

average layer thickness and, thus, shorter than the average distance for volume diffusion (see Fig. 1). Second, the effective area available for grain boundary diffusion is only a small fraction of the total area. Using the assumption of hexagonal grains (diagonal distance = d) and assuming that the grain boundary has a constant width (δ), the fraction of total area available for grain boundary diffusion is

$$f = \frac{\delta}{\sqrt{3}\mathrm{d}} \tag{4}$$

and the total flux due to grain boundary diffuison is

$$J_{\eta}^{GB} = -D_{\eta}^{GB} f \frac{\Delta C}{X_{AveGB}} \tag{5}$$

Then the total flux due to grain boundary and volume diffusion is

$$J_{\eta}^{Tot} = -\left\{ D_{\eta}^{VOL} \frac{\Delta C}{X_{Ave}} + D_{\eta}^{GB} \left(\frac{\delta}{\sqrt{3}\,\mathrm{d}} \right) \frac{\Delta C}{X_{AveGB}} \right\} \tag{6}$$

This expression may be simplified based on morphological observations. The diffusion distance for grain boundary diffusion is related to the layer thickness and the scallop geometry. As stated earlier, the η-phase grains remain nearly equiaxed as growth progresses. Grooves between the grains are likely due to a grain boundary grooving reaction. If grooving kinetics are sufficiently rapid, the wetting angle between grains would remain relatively constant. Therefore, it is reasonable to assume that the scallop shape remains fairly constant and only the dimensions grow. This would mean that the ratio

$$R = \frac{X_{AveGB}}{X_{Ave}} \tag{7}$$

may be nearly constant over time. Substituting this into the total flux expression above

$$J_{\eta}^{Tot} = -\left\{ D_{\eta}^{VOL} \frac{\Delta C}{X_{Ave}} + D_{\eta}^{GB} \left(\frac{\delta}{\sqrt{3}\,\mathrm{d}} \right) \left(\frac{1}{R} \right) \frac{\Delta C}{X_{Ave}} \right\} \tag{8}$$

or

$$J_{\eta}^{Tot} = -\left\{ D_{\eta}^{VOL} + D_{\eta}^{GB} \left(\frac{\delta}{\sqrt{3}\mathrm{d}} \right) \left(\frac{1}{\sqrt{R}} \right) \right\} \frac{\Delta C}{X_{Ave}} \tag{9}$$

For the intermetallic η-phase layers which develop during soldering:

- The grain size, d, is small,
- The typical grooves between grains are fairly deep such that typical R values are in the range of 0.15 to 0.4, and
- The temperatures involved in soldering (around 200°C) are moderate with respect to the melting temperature of the η-phase (peritectic temp. at 415°C).

All three of these factors favor grain boundary diffusion as the predominant mechanism for transport through the layers. Then, the total flux is approximately equal to the grain boundary flux alone.

$$J_{\eta}^{Tot} \approx -\left\{ D_{\eta}^{GB} \left(\frac{\delta}{\sqrt{3}\,\mathrm{d}} \right) \left(\frac{1}{R} \right) \right\} \frac{\Delta C}{X_{Ave}} \tag{10}$$

Using the equiaxed grain approximation leads to the substitution,

$$\mathrm{d} \approx X_{Ave} \tag{11}$$

and

$$J_{\eta}^{Tot} \approx -\left\{ D_{\eta}^{GB} \left(\frac{\delta}{\sqrt{3}\,X_{Ave}} \right) \left(\frac{1}{R} \right) \right\} \frac{\Delta C}{X_{Ave}} \tag{12}$$

or

$$J_{\eta}^{Tot} \approx -\left\{ D_{\eta}^{GB} \left(\frac{\delta\,\Delta C}{\sqrt{3}\,R} \right) \right\} \frac{1}{\left(X_{Ave}\right)^2} \tag{13}$$

Since diffusion along the grain boundary paths will be more rapid, Sn will accumulate at the interphase boundary adjacent to the η-η grain boundaries. Then, the Sn atoms will tend to redistribute laterally along the interphase boundary. One additional assumption will be made that the diffusivity along the interphase boundary is rapid enough to maintain a relatively planar interface at the ε–η and ε-Cu boundaries. This is in agreement with experimental observations in the literature and in the current study.

Accumulation of Sn at the η-Cu boundary is the driving force for the phase transformation which results in additional intermetallic layer growth. The average layer growth is directly proportional to the net flux over a particular area. Growth is related to volume of intermetallic compound created per mole of diffusant (V_{IM}). The growth rate (δX/δt) in terms of flux is then given by

$$\frac{\partial X}{\partial t} \propto -\left\{ D_{\eta}^{GB} V_{IM} \left(\frac{\delta \Delta C}{\sqrt{3}R} \right) \right\} \frac{1}{\left(X_{Ave}\right)^2} \tag{14}$$

For a constant soldering temperature, the diffusion coefficient, along with all the terms in brackets, are constant. Layer thickness as a function of time may then be determined by separating variables and integrating the above expression to obtain

$$\left(X_{Ave}\right)^3 \propto -\left\{ D_{\eta}^{GB} V_{IM} \left(\frac{\delta\,\Delta C}{\sqrt{3}\,R} \right) \right\} t + \left[X_{Ave}\left(\mathrm{at}\ t = t_i\right) \right]^3 \tag{15}$$

A more rigorous approach would require taking the initial thickness at the initial time, t_i when the intermetallic first forms a continuous layer (at about 10 s and a few tenths of a micron in thickness). As a first approximation, it will be assumed that initial layer thickness is zero at time t = 0.

$$\left(X_{Ave}\right)^3 \propto -\left\{ D_{\eta}^{GB} V_{IM} \left(\frac{\delta \Delta C}{\sqrt{3}R} \right) \right\} t \tag{16}$$

or

$$X_{Ave} \propto -\left\{ D_{\eta}^{GB} V_{IM} \left(\frac{\delta \Delta C}{\sqrt{3}R} \right) \right\}^{1/3} t^{1/3} \tag{17}$$

Thus, for intermetallic layer growth which is limited by grain boundary diffusion, in a system where the grains coarsen in proportion to the layer thickness, the layer thickness will follow a $t^{1/3}$ dependence on time.

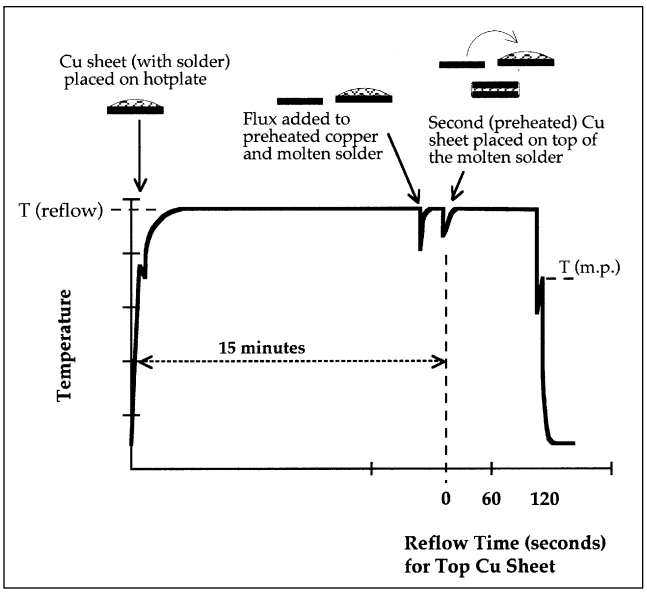

Fig. 4. Schematic temperature-time profile for an experiment to study intermetallic growth on Cu in contact with Cu saturated solder.

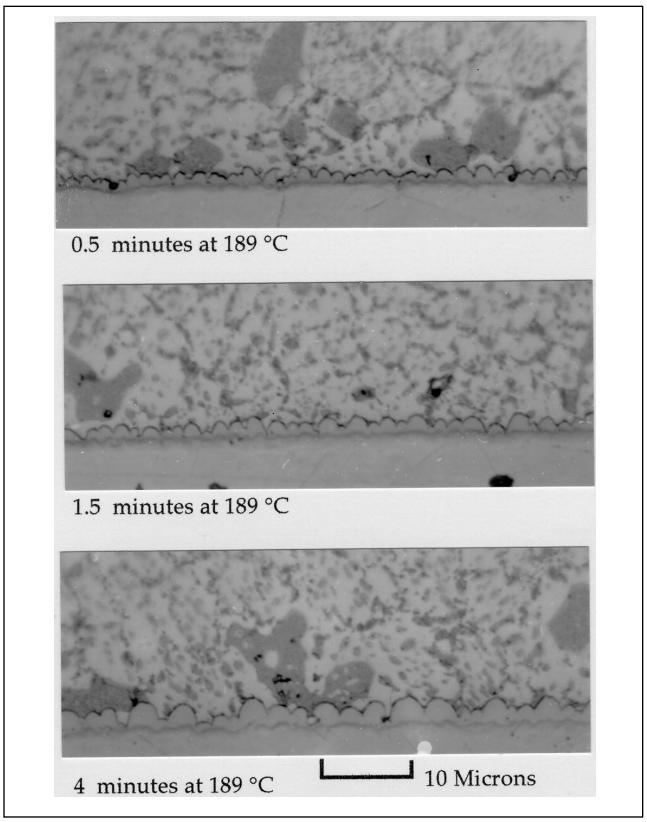

Fig. 5. Light micrographs for typical intermetallic layers formed during reflow at 189°C. The light gray scalloped regions are the Cu_6Sn_5 η-phase. A thin band of Cu_3Sn ε-phase is barely resolvable near the Cu substrate. In the photos, the solder is toward the top and the Cu substrate is toward the bottom.

EXPERIMENTAL PROCEDURE

Copper substrates for the isothermal soldering experiments were made from 1 mm thick cold-rolled Cu sheet of commercial purity (99.9+ % Cu). All specimens utilized commercial solder paste with a nominal

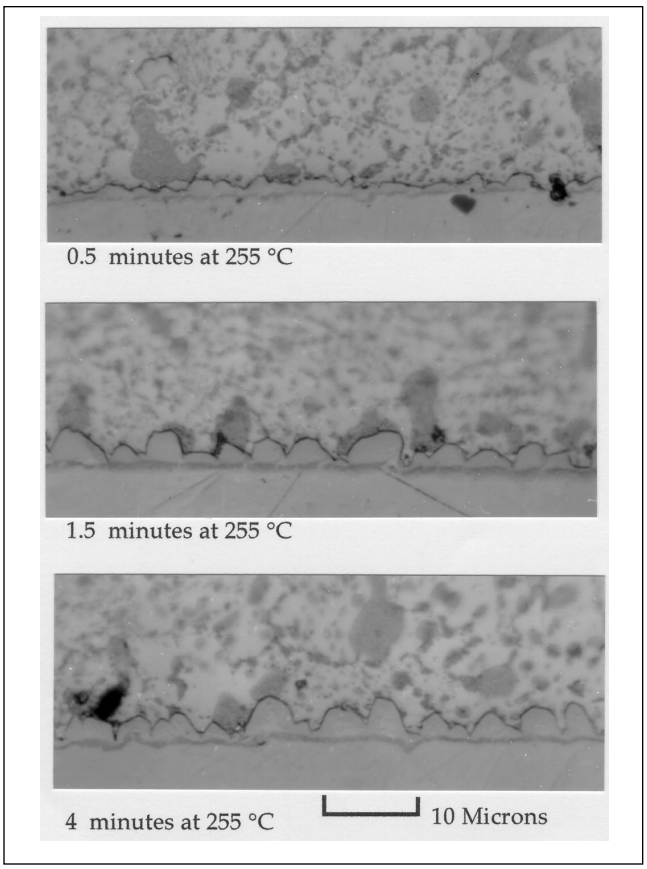

Fig. 6. Light micrographs for typical intermetallic layers formed during reflow at 255°C. The light gray scalloped regions are the Cu_6Sn_5 η-phase. A thin band of Cu_3Sn ε-phase is barely resolvable near the Cu substrate. In the photos, the solder is toward the top and the Cu substrate is toward the bottom.

composition of 62Sn - 36Pb - 2Ag (weight %). The surface of the Cu sheet was ground on a series of silicon carbide papers and polished with 1 μm alumina to produce a flat smooth surface. Just prior to reflow, the surfaces were dipped in a solution of 50% nitric acid in water for 5 s to remove any copper oxide and then rinsed in methanol.

Isothermal reflow experiments utilized a sandwich type sample consisting of a layer of solder in between two $5 \times 10 \times 1$ mm copper pieces. Three different reflow temperatures were used: 189, 255, and 310°C. A premeasured amount of solder paste (e.g., approximately 0.1 gram) was added to one of the $5 \times 10 \times 1$ mm Cu substrates. This sample was preheated at 160°C for 1 min and then transferred to a hot plate at the specified reflow temperature. The sample was held at this temperature for 15 min. Based on previous work, 15 min was sufficient to assure that the molten solder was essentially saturated with Cu.[21] Next, a second Cu strip was placed on the hot plate and preheated for 1 min. Then, a liquid activated rosin flux was put on the top surface of the second copper piece for 20 s. A small amount of flux was also put on the exposed solder to remove the tin oxide scale which had developed during the 15 min hold time. Finally, the second Cu piece was put on top of the saturated solder of the

first piece to complete the "sandwich." After specified times ranging from 30 s to 8 min, specimens were removed from the hot plate and cooled on a room temperature steel block (60 × 60 × 25 mm). Cooling was fast enough to suppress any additional intermetallic layer growth during solidification. A schematic temperature-time profile for this procedure is shown in Fig. 4. The samples were cross-sectioned and prepared for metallographic and SEM examination to determine intermetallic layer morphology and average layer thickness. Only the layer for the second (upper) Cu piece was evaluated. With this technique, the second Cu strip was in contact with Cu saturated solder from the very initial contact. Therefore, layer growth on this Cu strip should reflect only layer growth without the effects of dissolution of the intermetallic layer or the Cu strip.

In all cases, quantitative measurements of the intermetallic layer thickness were done using light micrographs taken of cross sections of the intermetallic layer. Photomicrographs were scanned into a Macintosh® computer using an Apple® OneScanner® optical scanner. The layer thicknesses in the scanned micrographs were evaluated using NIH Image© analysis software to measure the total area of intermetallic shown. Phase areas were divided by the length of boundary shown in the cross section to yield the average layer thickness. Reported values of thickness represent the average of four such measurements. Only the total intermetallic layer thickness is reported.

Several isothermal reflow samples were evaluated using a selective etching technique.[23] This technique involved immersing the samples in a solution of 35 gm per liter of ortho-nitrophenol and 50 gm per liter of NaOH in water at 80°C for approximately 30 min. This solution attacked the Pb phase very rapidly, removed the Sn phase more slowly and left the intermetallics and copper completely unaffected.

RESULTS AND DISCUSSION

Intermetallic Layer Morphology

Soldering experiments involved the reflow of samples for different lengths of time under near-isothermal conditions and in contact with solder which was saturated with Cu. The continuous layer of intermetallic on the copper substrate is composed of two phases: Cu_6Sn_5 (η-phase) adjacent to the solder and Cu_3Sn (ε-phase) adjacent to the copper. Figures 5 and 6 show a series of representative micrographs from samples reflowed at 189 and 255°C. The intermetallic layer is very rough and irregular. The interface between the η-phase and solder displays a scalloped morphology. The ε-phase layer is more uniform in thickness and is also more planar; however, it does to some extent follow the topography of the adjacent η-phase layer.

In order to aid in visualizing the morphology of the scalloped η-phase, a selective etching technique was utilized to remove the solder and expose the intermetallic layer. With this deep etching technique, the interfacial Cu-Sn intermetallic layer could be viewed in the SEM looking down from the solder side of the interface. The scalloped morphology of the intermetallic layer was clearly visible; the rounded grains and deep channels between the grains could be easily distinguished. Combining this technique with standard light microscopy of cross sections provided an excellent picture of the layer morphology. Figure 2 shows a series of representative photographs from samples soldered at 310°C. No quantitative measurements were made but qualitatively it appears that the lateral grain size is roughly equal to the layer thickness for both thin and thick layers.

Layer thickness increases with increasing reflow time. In addition, the size of the scallops increases with time. The increasing size of the scallops could be due to some combination of particle agglomeration[24] and ripening[19,20] or a competitive grain growth phenomenon. Within any one sample there is a variety of grain sizes. Some of this could be due to the fact that the cross sections cut through the scallops at different points; some are sectioned near the maximum scallop

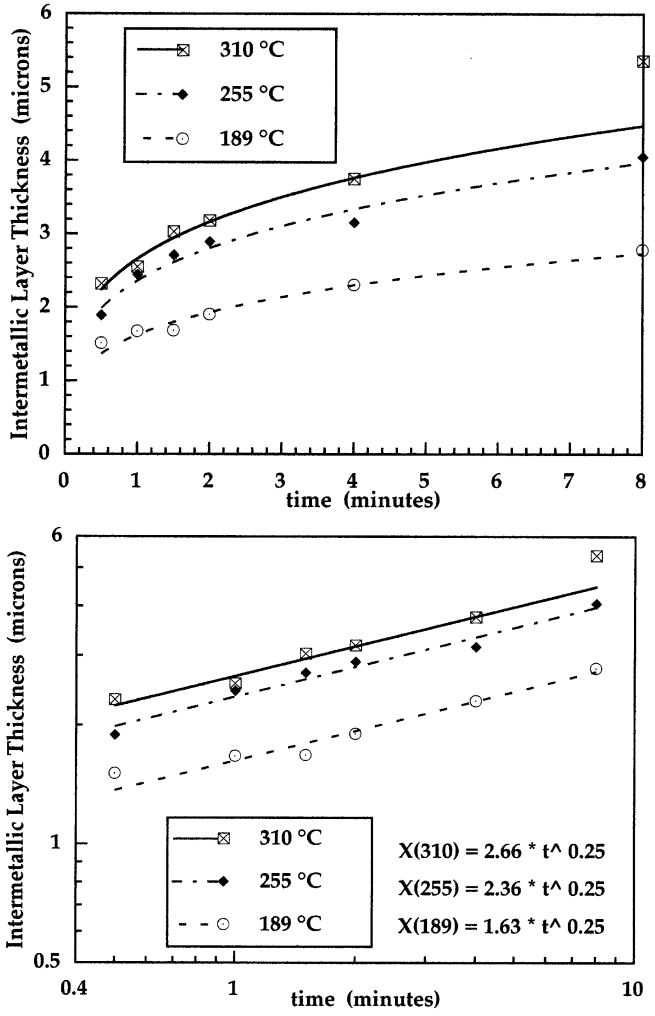

Fig. 7. Average intermetallic layer thickness vs time for isothermal reflow samples for which the solder was pre-saturated with dissolved copper. Data are plotted in both linear and log-log formats.

height while others are sectioned near the edge of a scallop. Also, the depth of the channels of solder between the grains appear to vary somewhat. On average, the layer thickness at these channels varies between 0.1 and 0.5 of the height of adjacent grains.

The channels (or grooves) between the η-phase grains are most likely due to a grain boundary grooving phenomenon. This interpretation is supported by the observation that these grooves exist regardless of the relative motion of the interface (receding with accompanying dissolution of intermetallic, advancing as with growth into a saturated liquid, or relatively stable as with slow growth and no dissolution).[21] Thus, the grooving is neither simply a growth-related phenomenon nor simply a dissolution related phenomenon. Grain boundary grooving is observed in solid-liquid couples as a result of thermodynamic considerations involving the energies of solid-solid (η-phase) and solid-liquid (η to molten solder) interphase boundaries. The groove angle is a function of the relative surface energies of a η-phase grain boundary, $\sigma_{\eta-\eta}$, and a solid-liquid interphase boundary, $\sigma_{\eta-\lambda}$, and results from a local balance of surface tension forces. For a particular pair of adjacent grains, it may be reasonable to assume that this wetting angle remains constant. However, the wetting angle depends on the relative mismatch in grain orientation and on the angle of the grain boundary relative to the solid-liquid interface. The observed grooving in these samples represents a variety of crystallographic conditions and, thus, it is expected that the groove angle would vary from one pair of grains to the next.

Growth Kinetics of Intermetallic Layer

Measured average layer thickness (including both η-phase and ε-phase layers) vs time are shown in Fig. 7. Analysis of the data shows that the isothermal growth kinetics may be adequately modeled with an empirical power law; for average thickness X, isothermal temperature T, and reflow time t:

$$X(t,T) = k_0 \exp\left(\frac{-A}{RT}\right) t^n \tag{18}$$

for
$$X(0,T) = 0 \tag{19}$$

The best fit parameters for the data were determined by setting up a least squares error analysis which simultaneously fit the three parameters, n, A and k_0. Results of the analysis were,

$$n = 0.25$$

and,
$$k_0 = \left(17.5 \tfrac{\mu m}{min^{0.25}}\right)$$

$$A = 9.0 \tfrac{kJoule}{mole}$$

The growth exponent from the experimental data, n = 0.25, indicates that the layer growth mechanism is not a simple diffusion limited process. This is not surprising in light of the irregular layer morphology and likely contribution of grain boundary diffusion. This result fits reasonably well with the growth model based on grain boundary diffusion and simultaneous coarsening as presented earlier in this paper. This model predicts a growth exponent of n = 0.33. Similar studies in the literature have reported growth exponents ranging from n = 0.21 to n = 0.37 for similar solid-liquid experiments.[1,16–18,20–22] The layer growth rate increases with increasing temperature and follows reasonably well with an Arrhenius relationship.

There are two possible explanations for the slightly lower exponent observed in the experiment. First, in the derivation, it was assumed that grain boundary diffusion predominates and volume diffusion could be neglected. At some point intermetallic grain size will grow large enough and the fraction of grain boundary area will be reduced enough that volume diffusion will take over as the predominant transport mechanism. This transition to a slower transport mechanism will tend to flatten out the latter part of the growth curve. As a result, the indicated growth exponent would be lower. It is possible that over the times and grain sizes typical for this experiment the system may be in transition from grain boundary controlled transport to volume diffusion controlled transport. Second, observed morphological trends used in the development of the model (i.e., equiaxed grains, constant ratio of channel thickness to average thickness) were approximated as simple constant ratios of grain size. These assumptions are valid only as a first approximation. Grain shapes seem to change slightly from spherical toward more elongated ellipsoidal shapes at the layer grows in thickness. This could influence the relative contribution of grain boundary diffusion. The relative depth of the channels may change over time.

As an example, the assumption for the ratio

$$R = \frac{X_{AveGB}}{X_{Ave}} \tag{20}$$

could be modified such that, instead of a constant ratio (R), the ratio changes as a function of grain size (using **r** to represent a variable ratio)

$$rX_{Ave} = \frac{X_{AveGB}}{X_{Ave}} \text{ or } r = \frac{X_{AveGB}}{X_{Ave}^2} \tag{21}$$

If this relationship is substituted in the previously shown development, the resulting growth law would be

$$X_{Ave} \propto -\left\{D_\eta^{GB}\left(\frac{\delta\Delta C}{\sqrt{3}r}\right)\right\}^{1/4} t^{1/4} \tag{22}$$

Activation Energy for Grain Boundary Diffusion

In order to evaluate the experimental data of the present study, it will be assumed that the growth model developed is essentially correct. Specifically, it will be assumed that the rate limiting mechanism for growth of thin layers is grain boundary diffusion through the η-phase layer and that the correct time exponent is n = 1/3. By comparing Eq. (17) and Eq. (18), it is evident that the empirical factor A is directly

related to the bracketed term in Eq, (17) as

$$k_0 \exp\left(\frac{-A}{RT}\right) \propto \left\{D_\eta^{GB} V_{IM}\left(\frac{\delta\Delta C}{\sqrt{3}R}\right)\right\}^{1/3} \quad (23)$$

It is reasonable to assume that ΔC is constant with respect to temperature since the phase boundaries for the η-phase are nearly vertical in the temperature range of interest. Assuming, also, that V_{IM}, ΔC, and R are constant with respect to temperature leads to the conclusion that the temperature dependence observed for the empirical factor A is due to the temperature dependence of the grain boundary diffusion coefficient

$$D_\eta^{GB} = D_{\eta 0}^{GB} \exp\left(\frac{-Q}{RT}\right). \quad (24)$$

If follows from these assumptions and from Eq. (23) that

$$\left\{k_0 \exp\left(\frac{-A}{RT}\right)\right\} \propto \left\{D_{\eta 0}^{GB} \exp\left(\frac{-Q}{RT}\right)\right\}^{1/3} \quad (25)$$

$$\exp\left(\frac{-A}{RT}\right) \propto \exp\left(\frac{-Q}{3RT}\right) \quad (26)$$

and $$3A = Q = 27 \frac{kJoule}{mole} \quad (27)$$

is the activation energy corresponding to grain boundary diffusion of Sn along the η-phase grain boundaries. This seems a reasonable activation energy for grain boundary diffusion. Previous experiments report an activation energy (presumably for volume diffusion) of 53 kJoule/mole for diffusion of Sn through the η-phase. No comparable data are available for grain boundary diffusion in the intermetallic.[6] It is generally true for metals that activation energy for grain boundary diffusion is about half that for volume diffusion.[25,26] While it is uncertain if a comparable relationship applies for intermetallic compounds, this general rule would indicate very good agreement between the literature and the current results.

CONCLUSIONS

A mathematical model was developed for predicting growth of an intermetallic compound layer during soldering of Sn based solder on copper. This growth model is based on diffusion through the η-phase layer as the rate limiting mechanism. Several typical assumptions were made including,

- Local equilibrium at the interphase boundaries,
- Negligible flux into the terminal phases, and
- Diffusion coefficients which are independent of composition.

Four additional assumptions were incorporated into the development in order to account for the fine-grained, scalloped intermetallic layer which develops during soldering. First, it was assumed that grain boundary diffusion is the predominant mechanism for transport through the layer. Fine intermetallic grain size, moderate temperatures, and the fact that the scalloped layer creates short diffusion paths through the layer at grain boundaries are three factors which support this assumption. Second, based on experimental observations, it was assumed that the intermetallic grains coarsen in such manner that the grains remain nearly equiaxed as they grow. This has the effect of reducing the availability of grain boundaries as diffusion paths as the intermetallic grows thicker. Third, it was assumed that the grains and the grooves between the grains maintain constant proportions at the layer grows. Fourth, it was assumed that the diffusion and growth for the η-phase layer is the predominant phenomenon and ε-phase growth may be treated simply as part of the Cu-to-Cu_6Sn_5 phase transformation. This model predicts that intermetallic layer growth should follow a $t^{1/3}$ dependence on time t.

Results from soldering experiments using Cu saturated 62Sn-36Pb-2Ag solder on Cu substrates agree reasonably well with the above model. The observed growth followed a $t^{0.25}$ dependence on time t. Growth rates followed an Arrhenius dependence on temperature in the range of 189 to 310°C. The lower growth exponent in the experiments as compared to the model could be due to a transition of the predominant transport mechanism from grain boundary diffusion to volume diffusion. As the layer grows thicker and grain coarsening progresses, the contribution of grain boundary diffusion will diminish. The transition to a slower transport mechanism would flatten out the latter part of the growth curve and result in a lower apparent growth exponent.

The experimental results were interpreted in terms of the model presented in this paper in order to estimate the activation energy for grain boundary diffusion. Activation energy for grain boundary diffusion was approximately 27 kJoule/mole. This is about half of the value reported in the literature for volume diffusion and, therefore seems reasonable for a grain boundary diffusion mechanism.

Further work could improve the present model. Several areas which require further study are:

- Acquire more accurate geometric details regarding the scallops and grooves in the intermetallic.
- Develop a means to incorporate a distribution of grain sizes and shapes instead of assuming uniform grain shape.
- Obtain improved estimates for the grain boundary diffusivity.

REFERENCES

1. D.R. Frear, *Solder Mechanics: A State of the Art Assessment*, eds. D.R. Frear, W.B. Jones and K.R. Kinsman, (Warrendale, PA: TMS, 1991), p. 191.
2. D.R. Frear, *JOM* 48 (5), 49 (1996).
3. D.R. Frear and P.T. Vianco, *Met. Trans. A* 25 (7), 1509 (1994).
4. J.K.Shang and D.Yao, *J. Electron. Packaging* 118 (3), 170 (1996).
5. A.J. Sunwoo, J.W. Morris, Jr. and G.K Lucey, Jr., *Met. Trans. A* 23 (4), 1323 (1992).

6. M. Onishi, and H. Fujibuchi, *Trans. JIM* 16, 539 (1975).
7. P.J. Kay and C.A. Mackay, *Trans. Inst. Met. Finishing* 54, 68 (1976).
8. A.D. Romig, Jr., Y.A. Chang, J.J. Stephens, D.R. Frear, V. Marcotte and C. Lea, *Solder Mechanics: A State of the Art Assessment*, eds. D.R. Frear, W.B. Jones and K.R. Kinsman, (Warrendale, PA: TMS, 1991), p. 29.
9. Y. Wu, J.A. Sees, C. Pouraghabagher, L.A. Foster, J.L. Marshall, E.G. Jacobs and R.F Pinizotto, *J. Electron. Mater*. 22 (7), 769 (1993).
10. K.L. Erickson, P.L. Hopkins and P.T. Vianco *J. Electron. Mater*. 23 (8), 729 (1994).
11. Z. Mei, A.J. Sunwoo and J.W. Morris, Jr., *Met. Trans. A* 23 (3), 857 (1992).
12. P.T. Vianco, P.F. Hlava and A.C. Kilgo, *J. Electron. Mater*. 23 (7), 721 (1994).
13. P.T. Vianco, K.L. Erickson and P.L. Hopkins, *J. Electron. Mater*. 23 (8), 721 (1994).
14. D. Unsworth and C. Mackay, *Trans. Inst. Met. Finishing* 51, 85 (1973).
15. H.K. Kim, H.K. Liou and K.N. Tu, *Appl. Phys. Lett*. 66 (18), 2337 (1995).
16. M. Schaefer, W. Laub, J.M. Sabee and R.A. Fournelle, *J. Electron. Mater.* 25 (6), 992 (1993).
17. S. Bader, W. Gust and H. Hieber, *Acta Met*. 43 (1), 329 (1995).
18. F. Bartels, J.W. Morris, Jr., G. Dalke and W. Gust, *J. Electron. Mater*. 23 (8), 787 (1994).
19. H.K. Kim and K.N. Tu, *Appl. Phys. Lett*. 67 (14), 2002 (1995).
20. H.K. Kim and K.N. Tu, *Phys. Rev. B* 53 (23), 16027 (1996).
21. M. Schaefer, W. Laub, R.A. Fournelle and J. Liang, *Design & Reliability of Solders and Solder Interconnections*, ed. R.K. Mahidhara, et al., (Warrendale, PA: TMS, 1997), p. 247.
22. J. London and D.W. Ashall, *Brazing & Soldering* 11, 49 (1986).
23. C. Lea, *A Scientific Guide to Surface Mount Technology*, (Ayr, Scotland: Electrochemical Publications, 1988), p. 329.
24. F. Bartels, Doctoral dissertation, Stuttgart, Germany: Institut Für Metallkunde der Universität Stuttgart und Max-Plank-Institut Für Metallforschung, 1993.
25. J.S. Kirkaldy, and D.J. Young, *Diffusion in the Condensed State*, (London: Institute of Metals, 1987).
26. I. Kaur, Y. Mishin and W. Gust, *Fundamentals of Grain and Interphase Boundary Diffusion*, (Chichester, England: John Wiley & Sons, 1995).